Journal of Visualization, Vol. 4, No. 3 (2001) 277-284

The Hemodynamic Study of the Cerebral Artery Using Numerical Simulations Based on Medical Imaging Data

Torii, R.*[1], Oshima, M.*[2], Kobayashi, T.*[2] and Takagi, K.*[3]

*1 School of Mechanical Engineering, The University of Tokyo, 7-3-1 Hongo, Bunkyo-ku, Tokyo 113-8656, Japan.
*2 Institute of Industrial Science, The University of Tokyo, 4-6-1 Komaba, Meguro-ku, Tokyo 153-8505, Japan.
*3 School of Medicine, Teikyo University, 2-11-2 Kaga, Itabashi-ku, Tokyo 173-8605, Japan.

Received 23 March 2001.
Revised 16 July 2001.

***Abstract*:** The paper aims to investigate effects of blood vessel geometry on hemodynamics of the cerebral artery, particularly the internal carotid artery using computer graphics. The medical statistics show that generation and rupture of the cerebral aneurysms is strongly correlated with the wall shear stress and flow patterns in the blood vessel. In order to provide better understanding of phenomena, the paper presents the numerical analysis system, which consists of pre-processing, simulation and post-processing. In the pre-processing, the medical imaging data, mainly CT (Computerized Tomographic) angiography, are used to construct the three-dimensional geometry of the artery. Various simulations are carried out varying curvature or location of bifurcation, and the results are visualized to investigate geometry effect.

***Keywords*:** cerebral aneurysm, computational hemodynamics, computed tomography

1. Introduction

It is known that over 90% of subarachnoid hemorrhage is caused by rupture of a cerebral aneurysm. The clinical statistics show that the generation of cerebral aneurysm has three characteristics: 1) there are three preferential areas where cerebral aneurysms are created (Karino et al.,1993), 2) the age group with a high risk of cerebral aneurysms is in 40's and 50's (Kuwahara et al.,1991), and 3) gender difference of generating rate exists. Particularly, women have higher tendency to have the cerebral aneurysm at a branch of ICA and PCom (see Fig. 1)

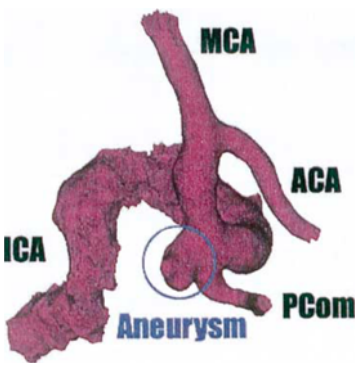

Fig. 1. Cerebral aneurysm at the bifurcation between internal carotid artery (ICA) and posterior communicating artery (PCom) extracted from CT angiography. MCA and ACA denotes middle and anterior cerebral arteries.

than men do. The difference in sex affects the size of skull, and the difference in age affects curvature of artery (Huber,1982). Considering these factors, the geometry of artery, which varies with age and sex, may play an important role in creation of the aneurysm.

To investigate influence of geometry, the system for the numerical analysis, which consists of pre-processing, numerical simulation and post-processing has been constructed. In this system, the real three-dimensional geometry of the artery is used for computational mesh, and measured transient velocity profile of blood flow is used for pulsatile inlet boundary conditions. Using this system, various simulations are carried out to analyze the effect of geometry of artery on wall shear stress distributions and flow patterns.

2. Numerical Analysis System

2.1 Mesh Generation

To calculate the flow in the real geometry of the artery, computational mesh was generated using CT imaging data (male in 70's). Figures 2 (a)-(c) show the slices of CT angiography. One slice consists of 512×512 pixels and each pixel has a 16 bit value corresponding to the brightness of color. There are a total of 100 frames with an interval of 0.4 mm in the vertical direction.

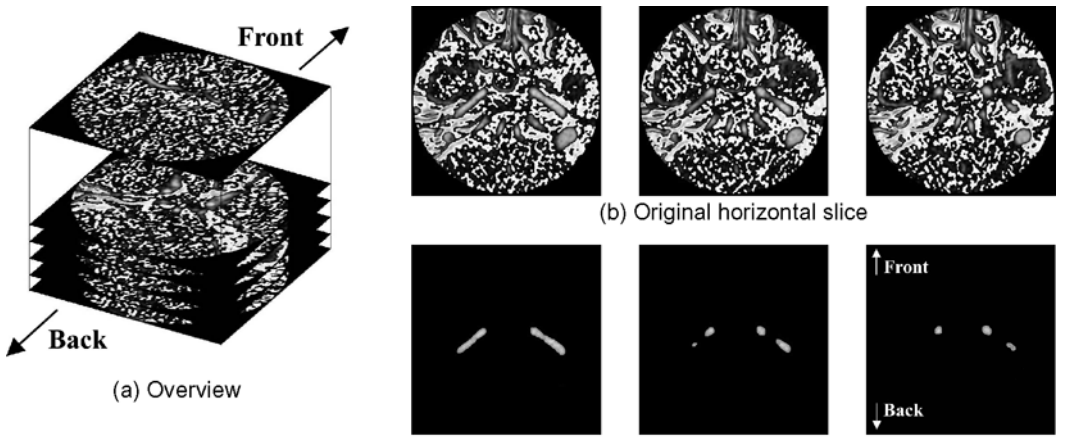

Fig. 2. CT angiography.

In order to construct the three-dimensional geometry from 100 pictures of the two-dimensional slice data, the iso-surface of the brightness of the color is created so as to depict the surface of the arterial wall. In this procedure, first of all, the area of ICA is extracted from original data as shown in Fig. 2 (c) in each horizontal CT slices. After the extraction of ICA geometry information, each slice is stacked up vertically to construct a three-dimensional geometry model such that the model surface corresponds to iso-surface of the brightness of the color. Then, the STL (STereo Lithography) data file is generated with triangular elements to describe the surface of ICA. This entire operation is executed using AVS, the commercial visualization software. After the STL data are

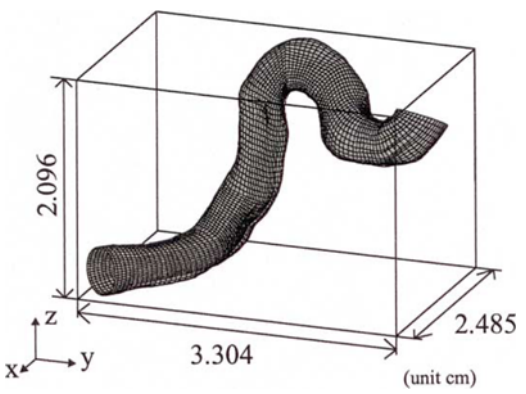

Fig. 3. Computational mesh.

transferred to the commercial meshing software, ICEM CFD, computational mesh for FEM (Finite Element Method) is created as shown in Fig. 3. The total number of elements is 38,860, and the total number of nodes is 42,120.

2.2 Computational Method

The blood flow in ICA is an incompressible flow and the flow can be treated as a laminar flow since the Reynolds number of blood flow is generally under 2,000 (Burleson et al.,1995) Thus, the governing equations are the continuity and Navier-Stokes equations. These equations are descretized by FEM. The numerical algorithm used in this calculation is summarized in Table 1.

Table 1. Numerical algorithm.

Element geometry	Hexahedral
Approximation function	1st order for velocity Piece-wise constant for pressure
Pressure and velocity coupling	MAC method
Solver of Poisson equation	Conjugate gradient method
Time integration	2nd order Adams-Bashforth method

2.3 Boundary Conditions

The boundary condition at the inlet is time-dependent pulsatile velocity profile called Womersley velocity profile (Taylor et al.,1998) which is given by the following equation for the axial component.

$$w(r,t) = \frac{2B_0}{pR^2}\left[1-\left(\frac{r}{R}\right)^2\right] + \sum_{n=1}^{N}\left\{\frac{B_n}{pR^2}\left[\frac{1-\dfrac{J_0\left(a_n\dfrac{r}{R}i^{3/2}\right)}{J_0\left(a_n i^{3/2}\right)}}{1-\dfrac{2J_1\left(a_n i^{3/2}\right)}{a_n i^{3/2}J_0\left(a_n i^{3/2}\right)}}\right]\right\}e^{inwt} \tag{1}$$

Here, R is the radius of inlet, J_0 and J_1 are Bessel functions of the first kind of order 0 and 1, respectively and $a_n = R\sqrt{nw/u}$ where u is the kinematic viscosity and w is the angular frequency of the cardiac cycle. Since the cross section of the inlet is not circular, an additional driving pipe with circular cross section is attached at the inlet. The nondimensional parameter $a = R\sqrt{w/u}$ is known as the Womersley number. Coefficients B_n are Fourier coefficients of flow rate, and are determined

$$Q(t) \approx \sum_{n=0}^{N} B_n e^{inwt} \tag{2}$$

Here, $Q(t)$ is the flow rate obtained by the ultrasound Doppler velocimetry, which is measured at the carotid artery of a male in 20's. And the order of series used in this calculation is ten. The flow rates of the measured velocity and of the Womersley velocity profile are shown in Fig. 4. The Womersley velocity profile shows good agreement with the measured velocity profile. Using this pulsatile velocity profile, the Reynolds number at the inlet varies from 160 to 850.

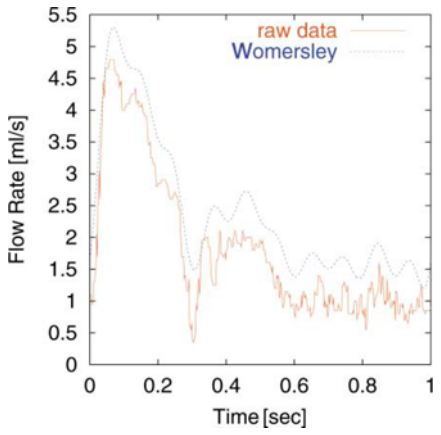

Fig. 4. Comparison of flow rate.

The boundary condition at the outlet of main artery and branching artery are traction free. In fact, outflow of the branching artery is almost zero because PCom is a bypath between ICA and PCA (Posterior Cerebral Artery). As a result of this calculation, outflow of the branching artery is very small, and is not larger than 0.25 m*l*/s (1/20 of outflow of main artery).

The boundary condition at the wall is non-slip. And the wall of the artery is assumed to be rigid. The initial condition is given by fully developed flow field at Re = 300.

2.4 Branching Model

Unfortunately, the branch of PCom from ICA, which is the high risk area of aneurysm, is not resolved in our CT angiography. In order to investigate effect of branching PCom numerically, the branching artery is modeled so as to emulate PCom. The diameter of the modeled PCom (d in Fig. 5) is about 1 mm, which is one fourth of ICA diameter. Since the location of bifurcation varies depending on individual cerebrovascular geometry, the modeled PCom is placed at these different locations as summerized in Table 2 and Fig. 5. The simulation is also conducted for ICA without the modeled PCom and the results of the four cases are compared. The modeled PCom consists of about 3,500 elements and 4,000 nodes.

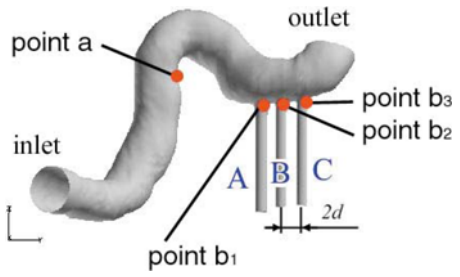

Fig. 5. Branching model (d indicates the diameter of branch).

Table 2. Computational models.

Case No.	Branching Point
1	no branch
2	A
3	B
4	C

3. Results

3.1 Characteristics of Averaged Wall Shear Stress

Using the present analysis system described in the previous section, we are able to perform one analysis within a week. Figure 6 shows the wall shear stress distributions averaged over one cardiac cycle. Since the magnitude of wall shear stress of artery is known to be between 10 to 70 dyne/cm^2 (Malek et al.,1999) the magnitude of the wall shear stress in these simulations shows good agreement with the actual value.

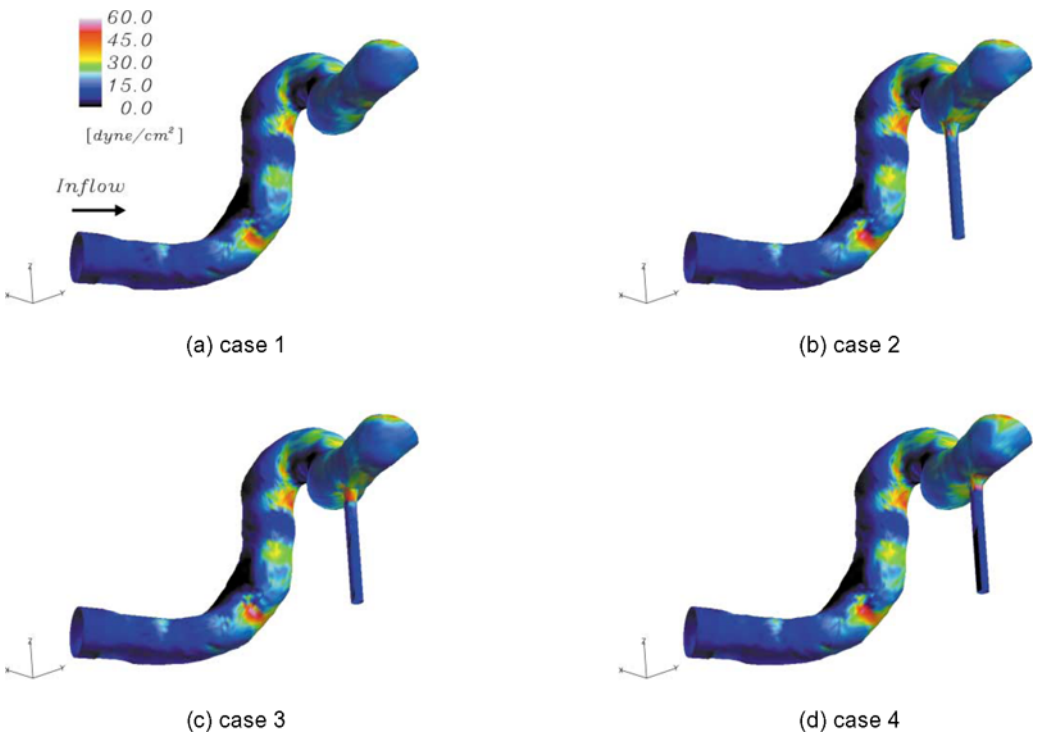

(a) case 1 (b) case 2

(c) case 3 (d) case 4

Fig. 6. Averaged wall shear stress distribution over one cardiac cycle.

Figure 6(a) shows that there are some areas where the wall shear stress concentrates even without a branching PCom. When there is the branching PCom, Figs. 6(b)-(d) show that the high wall shear stress area exists not only in the same area as case 1 but also on the wall near the branching PCom. The maximum wall shear stresses around branching area in cases 2-4 do not vary significantly, and are about 49(case 2), 48(case 3) and 48(case 4) dyne/cm^2 respectively.

Figures 7(a)-(c) show the secondary flow velocity distributions and wall shear stress distributions in the x-z and the y-z cross sections in cases 2-4. Each figure shows secondary flow. This secondary flow mainly consists of swirl, which is caused by the curvature located at the upstream of the branch. In cases 2 and 3, the secondary flow near the wall impinges on the wall of the branch as shown in Figs. 7(a) and (b). This causes the high wall shear stress near by the branching area in cases 2 and 3. On the other hand, in case 4, the secondary flow is not so strong in this area. Instead of the secondary flow, the axial flow near the wall impinges on the wall around the branching area.

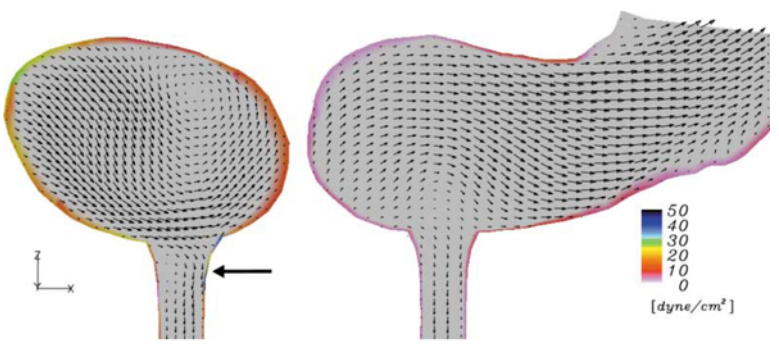

(a) case 2 (left: y = 2.46 cm, right: x = 1.40 cm)

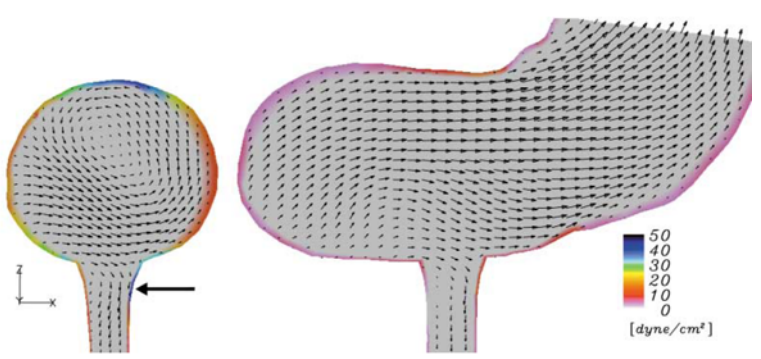

(b) case 3 (left: y = 2.68 cm, right: x = 1.46 cm)

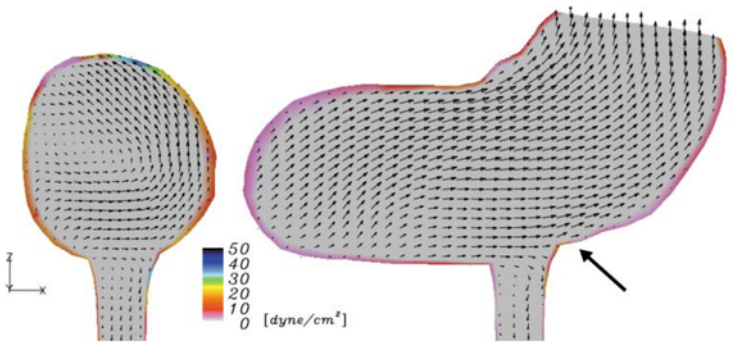

(c) case 4 (left: y = 2.84 cm, right: x = 1.52 cm)

Fig. 7. The secondary flow distribution around branching area averaged over one cardiac cycle. (The color contour shows the wall shear stress distribution, and arrows indicate the positions of the maximum wall shear stress, left: y-z plane, right: x-z plane).

Because of this difference in the direction of impinging flow, position of the maximum wall shear stress varies (see arrows in Fig. 7). In cases 2 and 3, position of maximum wall shear stress is on the wall of branch. But in case 4, position of maximum wall shear stress is very close to junction area, wall shear stress distribution in case 4 is probably affected by the way how the modeled PCom is connected to ICA, and this needs further investigation.

These results indicate that the wall shear stress around the branching area is highly affected by the flow approaching to the branch, which is caused by the complex and abrupt curvature of the artery. The location of the modeled PCom does not affect the distribution and the magnitude of the averaged wall shear stress.

3.2 Transient Behavior of Wall Shear Stress

Figure 8 describes the transient behavior of the wall shear stress at two points in each case. One is point a described in Fig. 5, where the averaged wall shear stress concentrates in all cases. The other point is around the branching area, where the maximum wall shear stress is observed for cases 2-4. In case 1, there is no PCom, but wall shear stress is recorded at a point where the modeled PCom branches out in case 3 (near point b_2 in Fig. 5).

This figure shows that the wall shear stress varies with a pulsatile motion of the heart. And the behavior of the wall shear stress in each case is similar to each other and is also quite similar to that of the flow rate at the inlet (see Fig. 4). This implies that at point a, the transient behavior of the wall shear stress is directly affected by the behavior of the flow at the inlet.

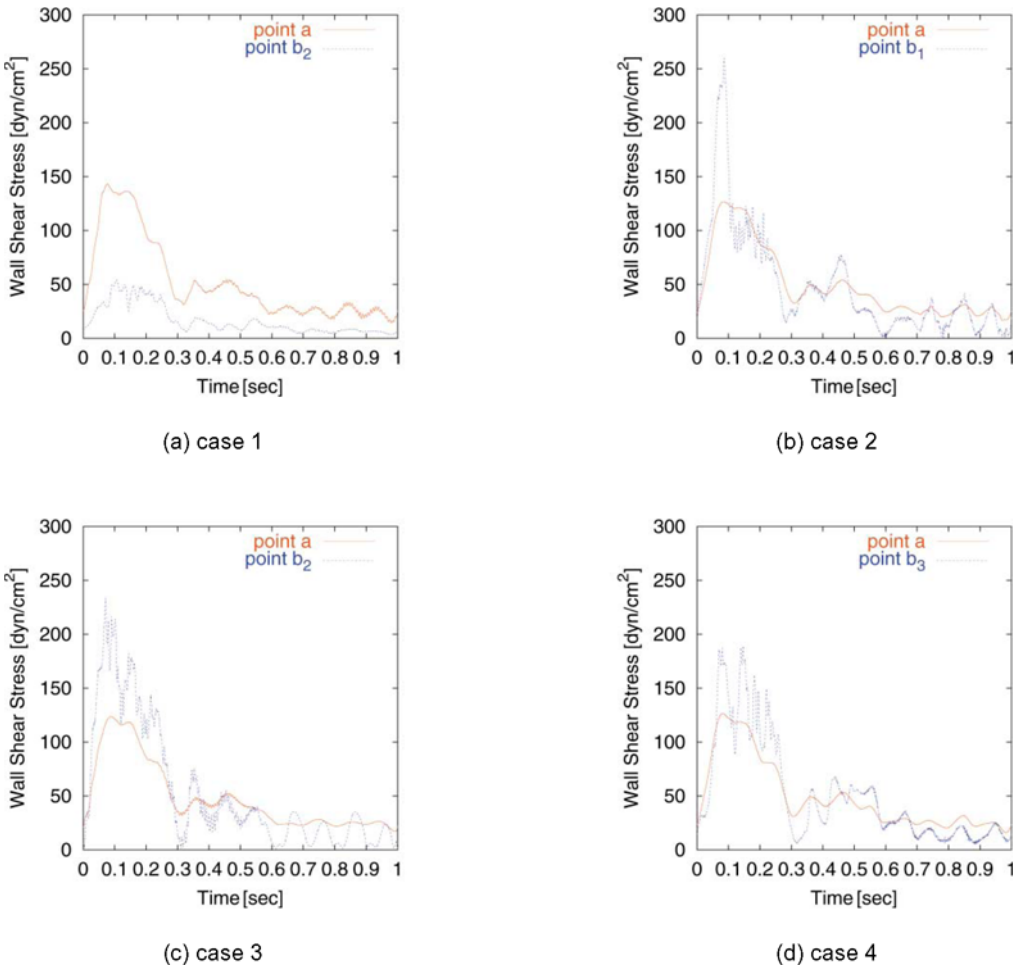

Fig. 8. Transient behavior of the wall shear stress at some points in cases 1-4 (the locations of points a and b_n are shown in Fig. 5).

On the other hand, at points b_1-b_3, the transient behavior of the wall shear stress is quite different from the behavior of the flow at the inlet. In the cases with the modeled PCom, the maximum magnitude of wall shear stress appears in the systole, and the magnitude is much larger than that in the case without branch. Furthermore, the transient behavior of wall shear stress distribution is different from the averaged one, and the magnitude of the wall shear stress at points b_1-b_3 is much larger than that at point a. The maximum magnitude, over 250 dyne/cm^2, is about four times as large as the usual value, 10-70 dyne/cm^2 (Malek et al.,1999).

From Figs. 8(b), (c) and (d), it is shown that the maximum magnitude of wall shear stress decreases as the position of branch moves further from the inlet. This is caused by difference in the characteristics of impinging flow in the branching area.

These results indicate that such an abrupt change in the wall shear stress may damage the arterial wall because the endothelial cell is known to be sensitive to the wall shear stress (Malek et al.,1999). This abrupt change of wall shear stress is mainly affected by combination of shape of artery upstream and position of branch.

4. Conclusions

The numerical analysis system based on medical imaging data is presented. The system can analyze one case study of the geometry within a week. In order to investigate effects of the geometry of artery on wall shear stress and flow pattern, the numerical simulations are performed. As a result, it is found that the distribution of the wall shear stress is dominantly affected by the relationship between the position of branch and the characteristics of flow approaching to the branching area. And the characteristics of flow is determined by complex curvature of ICA called "carotid siphon".

References

Burleson, A. C., Strother, C. M. and Turitto, V. T., Computer Modeling of Intracranialsaccular and Lateral Aneurysms of the Study of their Hemodynamics. Neurosurgery, Vol. 37, (1995), 774-783.

Huber, P., Cerebral Angiography -Internal Carotid Artery, (1982) Georg Thieme Verlag, New York.

Karino, T., Takeuchi, S., Kobayashi, N., Motomiya, M. and Mabuchi, S., Fluid dynamics in cerebrovascular diseases. Neurosurgeons, Vol. 12, (1993), 15-24, (in Japanese).

Kuwahara, T. and Fujitsu, K., Illustrated Neurosurgery, 2nd edition, (1991) , Nanzando, Tokyo, (in Japanese).

Malek, A. M., Alper, S. L. and Izumo, S., Hemodynamic Shear Stress and its Role in Atherosclerosis. JAMA, Vol. 282 (1999), 2035-2042.

Taylor, C. A., Hughes, T. J. R. and Zarins, C. K., Finite element Modeling of Blood Flow in Arteries. Comput. Methods Appl. Mech. Engrg, Vol. 26, (1998), 975-987.

Author Profile

Ryo Torii : He received his BSc (Eng Sci) degree in Mechanical Engineering Department in 1997 from Osaka University, and his MSc (Eng) degree in Mechanical Engineering Department in 1999 from The University of Tokyo, and currently is doing Ph.D program in The University of Tokyo. His research interest is numerical analysis in the field of cerebrovascular disease and blood flow.

Marie Oshima: She received her Ph.D in Nuclear Engineering Department, The University of Tokyo in 1992. Since her graduation, she has been working at Institute of Industrial Science, The University of Tokyo. She became an associate professor in 1999. She also worked at Stanford University as a visiting scholar from 1995 to 1996. Her specialities are computational fluid dynamics, particularly computational hemodynamics and the finite element analysis.

Toshio Kobayashi: He received his Ph.D in Mechanical Engineering Department, The University of Tokyo in 1970. Since completion of his Ph.D program, he has been a faculty member of Institute of Industrial Science, The University of Tokyo, and currently is a professor. His research interests are numerical analysis of turbulence, especially Large Eddy Simulation(LES), and Particle Imaging Velocimetry(PIV) technique. He is a member of The Science Council of Japan and serves as the President to the Japan Society of Mechanical Engineers(JSME), and Executive Vice President to International Federation of Automotive Engineering Societies(FISITA).

Kiyoshi Takagi: He works in Teikyo University School of Medicine as a neurosurgeon. He conducted basic biochemical studies of cerebral ischemia and etiological studies of cerebral aneurysm. Inspired from these studies, he is now interested in the relationship between the structure and function of the cerebral vasculature.